# Interaction of seismic background noise with oscillating pore fluids causes spectral modifications of passive seismic measurements at low frequencies

*Marcel Frehner\*, Department of Earth Sciences, ETH Zurich, frehner@erdw.ethz.ch, +41 44 632 88 72*
*Stefan M. Schmalholz, Department of Earth Sciences, ETH Zurich*
*Yuri Podladchikov, Physics of Geological Processes (PGP), University of Oslo*

## Summary

Studies of passive seismic data in the frequency range below 20Hz have shown that the frequency content of the ever-present seismic background noise changes above hydrocarbon reservoirs. Different explanations for this observation have been proposed. In this study, the effect of oscillating pore fluids, i.e. oil, on the seismic background noise is investigated. A non-wetting fluid drop entrapped in a pore can oscillate with a characteristic eigenfrequency. Capillary forces act as the restoring force driving the oscillations. A 1D wave equation is coupled with a linear oscillator equation, which represents these pore fluid oscillations. The resulting linear system of equations is solved numerically with explicit finite differences. The most energetic part of the seismic background noise, i.e. frequencies around 0.1-0.3Hz, is used as the external source. This part is presumably related to seismic surface waves generated by ocean waves. It is shown that the resulting elastic wave initiates oscillations of the fluid drops. The oscillatory energy of the pore fluid is transferred continuously to the elastic rock matrix. In consequence, seismic waves in the elastic rock carry a second frequency, the eigenfrequency of the pore fluid oscillations on top of the applied external frequency. Both frequencies can be measured at the earth surface. The presented model is considered as a possible explanation for observed spectral modifications above hydrocarbon reservoirs. Time evolution of the pore fluid oscillations seems to be related to the thickness of the hydrocarbon reservoir.

## Introduction

Spectral modifications of seismic background noise in the frequency range below 20Hz have been observed above hydrocarbon reservoirs (right gray bar in Figure 1) (Dangel et al., 2003; Bloch and Akrawi, 2006). A new direct hydrocarbon indication method was developed using spectra of low frequency seismic noise measurements. The physical explanation for these modifications is the subject of current discussions (Graf et al., 2007). Seismic attenuation phenomena in poro-elastic media, subsurface reflection patterns and phase transition effects (Suntsov et al., 2006) have been discussed as possible causes.

The behavior of non-wetting fluids entrapped in capillary tubes and in idealized pore spaces were thoroughly studied in the past (Dvorkin et al., 1990; Graham and Higdon,

2000a, 2000b). The main finding of these studies is the oscillatory movement of fluids when an external force is applied. The frequencies of these oscillations can be reasonably low. The driving force is the surface tension force acting on the interface between the wetting and the non-wetting fluid phase. The results of these works were used by the oil and gas industry to develop a new enhanced oil recovery (EOR) method termed "wave stimulation of oil" or "vibratory mobilization" (Iassonov and Beresnev, 2003; Beresnev et al., 2005; Li et al., 2005). The general idea of the method is to excite oscillations of the entrapped oil with a vibratory device. Inertial forces occurring with oscillations eventually are strong enough to overcome the capillary pressure. This way the oil drops are enabled to leave the pore constrictions. The method and many application results are reviewed in Beresnev and Johnson (1994). Biot (1962) and many following publications consider fully saturated porous rocks where no oscillations can take place. The main focus of these publications is to better understand the dynamics of the second or slow P-wave that is a special feature of Biot's poro-elastic theory. Pore fluid oscillations considered in the presented work only occur in partially saturated rocks. The effect of these oscillations on seismic waves traveling through a porous rock is investigated together with the effect they cause at the earth surface. Naturally induced oscillations are considered that are generated by the ever-present seismic background noise.
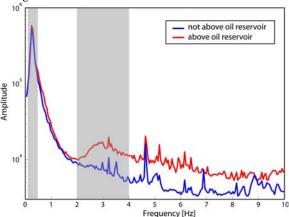


Figure 1: Field measurements of seismic background noise. One measurement above (red) and one nearby (blue) a proven oil reservoir. Left gray bar: Ocean-wave peak; Right gray bar: Modification due to reservoir. Spectraseis survey for Petrobras, Potiguar Basin, Brazil, 2004

**Methods**

<u>Coupling between pore fluid oscillations and elastic rock</u>
Various theoretical investigations showed that a non-wetting fluid drop, i.e. oil, entrapped in a capillary tube can oscillate (Hilpert et al., 2000; Beresnev, 2006; Graham and Higdon, 2000a, 2000b). Both sliding and pinned contact lines were considered. In both cases the radii of the menisci change when the fluid drop is displaced out of its equilibrium position. In the case of sliding contact lines a variable width of the capillary tube has to be assumed to obtain the change of radii. This change of radii of the menisci changes the capillary pressure at the corresponding menisci which leads to a restoring force that drives the oscillation. Hilpert et al. (2000) demonstrated a resonant behavior of such oscillations and Holzner et al. (2007) showed that possible eigenfrequencies range down to reasonably low values (<10Hz). For simplicity, oscillations of pore fluids in this work are approximated with a linear one-dimensional oscillator model with the eigenfrequency $\omega_0$. The eigenfrequency of the oscillations are assumed to be constant for all pores. The pore fluid oscillations are coupled to a one-dimensional linear elastic solid. A sketch of the rheological model is given in Figure 2. The beam on the left hand side represents a one dimensional linear elastic solid which is coupled to a one dimensional linear oscillator. The oscillations influence the behaviour of the elastic solid and vice versa. In the continuous limit of an infinite number of pore fluid oscillators the total kinetic energies $E_{kin}$ and total potential energies $E_{pot}$ of the fluid and solid subsystems are given by

$$E_{kin}^f = \frac{1}{2}\int_0^l S\phi\rho^f \left(\dot{u}^f\right)^2 dx \,,\, E_{kin}^s = \frac{1}{2}\int_0^l (1-\phi)\rho^s \left(\dot{u}^s\right)^2 dx$$

$$E_{pot}^f = \frac{1}{2}\int_0^l S\phi\rho^f \omega_0^2 \left(u^f - u^s\right)^2 dx \,,\, E_{pot}^s = \frac{1}{2}\int_0^l \sigma^s \varepsilon^s dx \qquad (1)$$

Superscript $f$ and $s$ denote fluid and solid parts of the system, respectively. $u^i$ are displacements and $\dot{u}^i$ are their time derivatives. $l$ is the total length of the one-dimensional model. $\phi$ is porosity of the elastic rock and $\rho^f$ and $\rho^s$ is fluid and solid mass density, respectively. $S$ is the filling level of the pores and is a number between 0 and 1. $\sigma^s$ is the stress in the elastic rock and $\varepsilon^s$ is the strain, i.e. spatial derivative of solid displacement. Stress and strain are linearly related, i.e. a linear rheology is assumed for the solid. Non-connected pores are assumed that do not allow pressure waves to propagate in the fluid. Equations (1) only consider the solid and fluid subsystems. When the filling level of the pores $S$ is smaller than 1, a third phase is present in the system. Here it is assumed to be a gaseous phase. Both its kinetic and potential energy is small compared to the fluid and solid phases and is neglected. For the continuous two-component system Hamilton's variational principle can be applied to the Lagrangian functional $L$ (Fetter and Walecka, 1980).

$$\delta \int_{t_1}^{t_2} L\,dt = \delta \int_{t_1}^{t_2} (T-U)\,dt = \int_{t_1}^{t_2}\int_0^l \delta\mathcal{L}\,dx\,dt \qquad (2)$$

$T$ and $U$ are total kinetic and total potential energies of the coupled system, respectively. $t_1$ and $t_2$ are two points in time. $\mathcal{L}$ is the Lagrangian density and has dimension of energy per unit length. Assuming small variations Equation (2) splits into two equations for the solid and fluid. Partial integration is carried out omitting the resulting boundary terms by applying zero-boundary conditions. Variations $\delta u^i$ arise as common multipliers for all terms. Since variations are arbitrary the remaining terms have to be equal to zero. The resulting equations are the Euler-Lagrange equations for the continuous two-component system.

$$\frac{\partial \mathcal{L}}{\partial u^i} - \frac{d}{dt}\left(\frac{\partial \mathcal{L}}{\partial \dot{u}^i}\right) - \frac{d}{dx}\left(\frac{\partial \mathcal{L}}{\partial \varepsilon^i}\right) = 0 \qquad (3)$$

The Lagrangian density $\mathcal{L}$ (Equation 2) is substituted into the Euler-Lagrange equations. The final equations of motion result.

$$S\phi\rho^f \frac{\partial^2 u^f}{\partial t^2} = -S\phi\rho^f \omega_0^2 \left(u^f - u^s\right)$$

$$(1-\phi)\rho^s \frac{\partial^2 u^s}{\partial t^2} = \frac{\partial}{\partial x}\left(E\frac{\partial u^s}{\partial x}\right) + S\phi\rho^f \omega_0^2 \left(u^f - u^s\right) \qquad (4)$$

The first of Equations (4) is almost identical to a linear one-dimensional oscillator equation. It differs in the sense of its formulation in terms of relative displacement and averaged density ($S\phi\rho^f$). The left hand side together with the first term of the right hand side of the second of Equations (4) is similar to a one-dimensional wave equation (Szabo, 1985). It is also written in terms of the averaged density (($1-\phi)\rho^s$). The additional term on the right hand side is also written in terms of relative displacement and links the fluid and the solid motion.
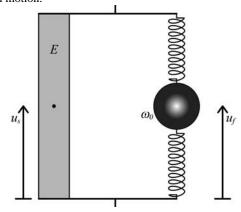


Figure 2: Schematic rheological model for coupling between elastic deformation and pore fluid oscillations. Elastic bar with Young's modulus $E$ is coupled with a linear oscillator of eigenfrequency $\omega_0$. Two displacements have to be considered, one for the elastic subsystem $u_s$ and one for the oscillatory fluid subsystem $u_f$.

# Seismic noise and pore fluid oscillations

<u>Numerical methods and setup</u>

Using two kinematic equations for $u^f$ and $u^s$ and the constitutive equation, Equations (4) are expanded to five first order linear partial differential equations. They are discretized using the finite difference method on a one-dimensional staggered grid (Virieux, 1986). Discretization in time is done explicitly with a predictor-corrector method. Boundary conditions can be rigid (all velocities equal Zero) or non-reflecting (Ionescu and Igel, 2003) (Figure 3). Three receivers are placed in the model together with an external source at the position of receiver $R_1$. Since the model is one-dimensional and the layers on top and at the bottom are linear elastic, the distances of $R_1$, $R_3$ and S from the porous layer do not change character of the recorded signal apart from adding a time shift. Therefore these distances are chosen to be small (7m) to optimize numerical resolution. The source term is added to the second of Equations (4) and acts as an additional force. The Fourier spectrum of a typical measurement of seismic noise shows a very distinct peak at around 0.1-0.3Hz (left gray bar in Figure 1). This high energy spectral peak is a global feature that can be measured everywhere in the world. It is presumably related to seismic surface waves generated by ocean waves (Aki and Richards, 1980). In this study, seismic background noise is reduced to this most energetic frequency. The external source term in Equation (4) becomes

$$F(x,t) = A_0(x)\sin(\Omega t) \quad \begin{array}{l} A_0(x) = 0 \ for \ x \neq x_{source} \\ A_0(x) = 1 \ for \ x = x_{source} \end{array} \quad (5)$$

$\Omega = 1.89 \ (= 0.3\text{Hz} \cdot 2\pi)$. The external source is applied at one point $x_{source}$ in the model domain. The eigenfrequency of the pore fluid oscillations is fixed to 3Hz throughout the model domain according to Holzner (2007). Physical parameters used in the simulations are given in Table 1.



Figure 3: 1D model setup for numerical simulations consists of three receivers $R_1$-$R_3$ and one source S identical with position of receiver $R_1$. Shaded area (i.e. the reservoir) is described by coupled system of Equations (4), the rest is purely elastic. Lower and upper boundaries can be rigid (zero displacement) or non-reflecting.

| Symbol | Value |
|--------|-------|
| $\omega_0$ | 18.85 (=3Hz · 2π) |
| $\rho^f$ | 800 kg m$^{-3}$ |
| $\rho^s$ | 2800 kg m$^{-3}$ |
| $E$ | $2 \cdot 10^{10}$Pa |
| $\phi$ | 0.3 |
| $S$ | 0.9 |
| $\Omega$ | 1.89 (=0.3Hz · 2π) |

Table 1: Values used in numerical simulations. Parameters not listed are explained in the text.

**Numerical results**

<u>Energy conservation and transfer</u>

For a first simulation only the 120m thick shaded area, i.e. the reservoir, of the model in Figure 3 was used without the elastic layers and with two rigid boundaries. No source was applied, but a Gaussian curve for the solid velocity was used as initial condition. Figure 4 shows the time evolution of the four energies (thin lines) in the system (Equations 1). Also, the total fluid energy and the total solid energy are shown together with the total energy of the system (thick lines). The energies of the solid and fluid phase always add up to constant total system energy, i.e. the total energy is conserved. At the same time energy is transferred back and forth between the solid and the fluid subsystems. The beginning with zero energy of the fluid represents the initial conditions. That the oscillations of the different energy contributions over time happen with similar amplitudes shows that the pore fluid oscillations influence the behavior of the solid phase considerably.
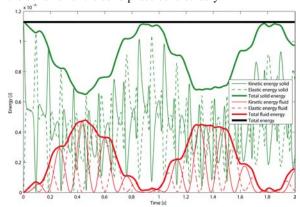


Figure 4: Time evolution of the four different energies in the system. A 120m thick homogeneous system with two rigid boundaries is used. No external source is applied but an initial velocity perturbation in the solid. The total energy stays constant over time, i.e. energy is conserved.

<u>Spectra over time for different reservoir thicknesses</u>

Several numerical simulations with different reservoir thicknesses were performed. At receiver $R_3$ a Fourier spectrum was calculated with the recorded solid velocity after different simulation lengths. Figure 5 shows the evolving Fourier spectrum for the case of a 50m thick porous layer. The amplitude of the peak at 0.3Hz stays constant over time while the amplitudes of all other frequencies, including 3Hz, decrease. The decrease of the spectral amplitude at the eigenfrequency of the pore fluid oscillations is different for different thicknesses of the reservoir. Figure 6 shows the time evolution of the ratio between the spectral amplitudes of the 3Hz-peak and the 0.3Hz-peak. A thick reservoir initially creates higher amplitudes of the spectral peak at 3Hz. This amplitude decreases linearly with time on double-logarithmic axes. A

thin reservoir initially creates lower amplitudes of the spectral peak at 3Hz. The decrease with time is smaller until the amplitude asymptotically reaches the values for thicker reservoirs. A saturation of this effect occurs at a thickness of around 70m.
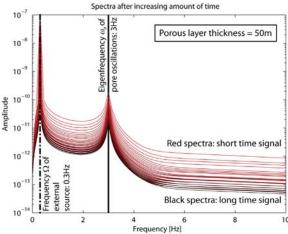


Figure 5: Spectra of solid velocity at receiver $R_3$ for a 50m thick reservoir. Different spectra are calculated after different simulation lengths. Longest time signal is 120s (black spectra), shortest is 3.5s (red). Dash-dotted vertical line: Frequency of external force; Solid vertical line: Eigenfrequency of pore fluid oscillations.
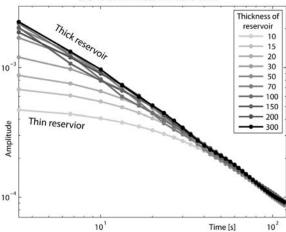


Figure 6: Time evolution of the amplitude ratio between 3Hz-peak and 0.3Hz-peak in the spectra in double-logarighmic representation. Different colors represent different reservoir thicknesses. Spectra are calculated with the solid velocity at receiver $R_3$.

## Discussion

Despite Equations (4) are linear. Still, the monochromatic external source (Equation 5) acting on the solid phase excites the pore fluid to oscillate with its eigenfrequency. These oscillations are initiated by the incident elastic wave.

While the wave itself is monochromatic, the wave front contains all frequencies, including the eigenfrequency of the pore fluid oscillations. After the wave front has passed, the pore fluid continues to oscillate with its eigenfrequency $\omega_0$ and constantly transfers energy to the elastic porous matrix. This results in a decrease of the amplitude of the oscillations.

For further studies two types of non-linear oscillators were used to describe pore fluid oscillations. These non-linearities result from complex pore geometries and compressibility assumption. Preliminary results show that non-linearities have only a small effect on the energy transfer from pore fluids to solid.

To have models with a more realistic external source, the low frequency part (<0.7Hz) of real passive measurements of seismic background noise will be used in the numerical model. The resulting source is nearly monochromatic but with strongly varying amplitudes over time. This amplitude variation acts like many incident wave fronts. Presumably, oscillations of pore fluids are more excited than in the case with only one incident wave front. The peak at the eigenfrequency of pore fluid oscillations in the solid spectra is expected to be more pronounced. Additional numerical simulations will be performed with the reservoir having lower impedance than the elastic surrounding. Standing waves within the reservoir may develop. They are expected to excite the pore fluid oscillations more than in the case without impedance contrast.

Natural porous rocks contain a range of pore sizes which leads to varying eigenfrequencies of the fluid oscillations. Observed low frequency spectral modifications of seismic background noise (right gray bar in Figure 1) may be explained as a superposition of several spectral peaks around 3Hz created by pore fluid oscillations with different eigenfrequencies.

## Conclusions

The presented model demonstrates the possibility of coupling between pore fluid oscillations and elastic wave propagation. The micro-scale pore fluid oscillations are able to change the frequency content of the large-scale elastic wave in the low frequency range. For explaining observed spectral modifications of seismic background noise above hydrocarbon reservoirs, oscillations of oil entrapped in pore constrictions must be considered.

## Acknowledgements

**EDITED REFERENCES**
Note: This reference list is a copy-edited version of the reference list submitted by the author. Reference lists for the 2007 SEG Technical Program Expanded Abstracts have been copy edited so that references provided with the online metadata for each paper will achieve a high degree of linking to cited sources that appear on the Web.

**REFERENCES**

Aki, K., and P. G. Richards, 1980, Quantitative seismology: Theory and methods: W. H. Freeman and Company.

Beresnev, I. A., 2006, Theory of vibratory mobilization on nonwetting fluids entrapped in pore constrictions: Geophysics, 71, no. 6, N47–N56

Beresnev, I. A., and P. A. Johnson, 1994, Elastic-wave stimulation of oil production - a review of methods and results: Geophysics, 59, 1000–1017.

Beresnev, I. A., R. D. Vigil, W. Q. Li, W. D. Pennington, R. M. Turpening, P. P. Lassonov, and R. P. Ewing, 2005, Elastic waves push organic fluids from reservoir rock: Geophysical Research Letters, 32.

Biot, M. A., 1962, Mechanics of deformation and acoustic propagation in porous media: Journal of Applied Physics, 33, 1482–1498.

Bloch, G., and K. Akrawi, 2006, Application of low frequency passive seismic surveys in ADCO, UAE: Passive Seismic Workshop, EAGE.

Dangel, S., M. E. Schaepman, E. P. Stoll, R. Carniel, O. Barzandji, E. D. Rode, and J. M. Singer, 2003, Phenomenology of tremor-like signals observed over hydrocarbon reservoirs: Journal of Volcanology and Geothermal Research, 128, 135–158.

Dvorkin, J., G. Mavko, and A. Nur, 1990, The oscillations of a viscous compressible fluid in an arbitrarily-shaped pore: Mechanics of Materials, 9, 165–179

Fetter, A. L., and J. D. Walecka, 1980, Theoretical mechanics of particles and continua: McGraw-Hill Book Company.

Graf, R., S. M. Schmalholz, Y. Podladchikov, and E. Saenger, 2007, Passive low frequency spectral analysis: Exploring a new field in geophysics: World Oil, 47–52

Graham, D. R., and J. J. L. Higdon, 2000a, Oscillatory flow of droplets in capillary tubes. Part 1. Straight tubes: Journal of Fluid Mechanics, 425, 31–53

———, 2000b, Oscillatory flow of droplets in capillary tubes. Part 2. Constricted tubes: Journal of Fluid Mechanics, 425, 55–77

Hilpert, M., G. H. Jirka, and E. J. Plate, 2000, Capillarity-induced resonance of oil blobs in capillary tubes and porous media: Geophysics, 65, 874–883.

Holzner, R., P. Eschle, S. Dangel, M. Frehner, C. Narayanan, and D. Lakehal, 2007, Hydrocarbon microtremors interpreted as nonlinear oscillations driven by oceanic background waves: Communications in nonlinear science and numerical simulation.

Iassonov, P. P., and I. A. Beresnev, 2003, A model for enhanced fluid percolation in porous media by application of low-frequency elastic waves: Journal of Geophysical Research-Solid Earth, 108

Li, W. Q., R. D. Vigil, I. A. Beresnev, P. Iassonov, and R. Ewing, 2005, Vibration-induced mobilization of trapped oil ganglia in porous media: Experimental validation of a capillary-physics mechanism: Journal of Colloid and Interface Science, 289, 193–199

Suntsov, A. E., S. L. Aroutunov, A. M. Mekhnin, and B. Y. Meltchouk, 2006, Passive infra-frequency microseismic technology – experience and problems of practical use: Passive Seismic Workshop, EAGE.

Szabo, I., 1985, Höhere technische mechanik: Springer-Verlag.

Virieux, J., 1986, P-Sv-wave propagation in heterogeneous media - velocity-stress fnite-difference method: Geophysics, 51, 889–901